

AD-A101 550

FOREIGN TECHNOLOGY DIV WRIGHT-PATTERSON AFB OH

ACTA MECHANICA SINICA (SELECTED ARTICLES), (U)

JUN 81 K CHO, C S TAO, X ZENG

UNCLASSIFIED FTD-ID(RS)T-0304-81

F/6 5/1

NL

[1 of]  
AC  
AD-550

END  
DATE  
FILED  
8-88  
OTIC

ADA101550

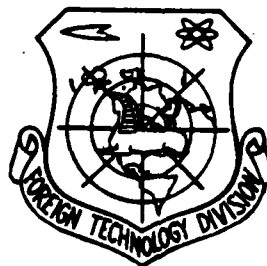
FTD-ID(RS)T-0304-81



## FOREIGN TECHNOLOGY DIVISION



ACTA MECHANICA SINICA  
(Selected Articles)



Approved for public release;  
distribution unlimited.



81 7 17 063

FTD -ID(RS)T-0304-81

## EDITED TRANSLATION

(14) FTD-ID(RS)T-0304-81

11 23  
26 Jun 1981

MICROFICHE NR: FTD-C-81-000578

60 ACTA MECHANICA SINICA (Selected Articles)

English pages: 20

Source: ~~Edited from~~ Acta Mechanica Sinica, Nr. 2, 1980,  
pp. 129-137

10  
Kao / Cho  
Chao Shu / Tao  
Zhang Xin-Chuan

Country of origin: (China)

Translated by: SCITRAN

F33657-78-D-0619

Requester: FTD/TQTA

Distribution limited to U. S. Government Agencies  
Only; Proprietary (Copyright) Information; Other  
requests for this document must be referred to  
FTD/STINFO.

THIS TRANSLATION IS A RENDITION OF THE ORIGINAL FOREIGN TEXT WITHOUT ANY ANALYTICAL OR EDITORIAL COMMENT. STATEMENTS OR THEORIES ADVOCATED OR IMPLIED ARE THOSE OF THE SOURCE AND DO NOT NECESSARILY REFLECT THE POSITION OR OPINION OF THE FOREIGN TECHNOLOGY DIVISION.

PREPARED BY:

TRANSLATION DIVISION  
FOREIGN TECHNOLOGY DIVISION  
WP-AFB, OHIO.

FTD-ID(RS)T-0304-81

Date 26 Jun 19 81

## TABLE OF CONTENTS

The Theory of Gain, Intensity and Power of Gas Lasers, by Kao Cho and Chao Shu Tao.....	1
Contact Problems of Long Rigid Frame Footing on Elastic Foundation, by Zeng Xin-Chuan.....	15

Accession No.	
NTIS	.....
DTIC	.....
U.S. No.	.....
Joint	.....
By.....	
Distribution/	
Availability Codes	
Avail	and/or
Dist	Special
A	

THE THEORY OF GAIN, INTENSITY AND POWER  
OF GAS LASERS

Kao Cho\* and Chao Shu Tao

ABSTRACT

The particle thermal velocity distribution is introduced into the speed equation to obtain the relations between gain, intensity and power of gas lasers. This paper reached the same conclusions as reference [1] under uniform broadening conditions. The results were simplified to become the well known non-flowing gas laser equations when the flow speed is zero.

In the analysis, the change in the reflectivity of the mirror and the degree of excitation as a function of time of gases in the upstream region of the optical chamber were considered with respect to both continuous and pulsed gas-flowing  $\text{CO}_2$  lasers.

I. INTRODUCTION

In the analysis of a gas-flowing  $\text{CO}_2$  laser, under the conditions that gain is equal to consumption, the solution to the speed equations put on line [1,2] applies only to the uniform broadening situation. Under conditions that both uniform and non-uniform broadenings exist, reference [3] made an analysis. In addition, the semi-empirical analyses of gas flow lasers [4,5] suggested that it was possible to apply some theory in the treatment of non-flow gas lasers in the explanation of experimental results with gas flow lasers. However, theoretical results were already available [1-3] for gas flow lasers. But they cannot be reduced to

\*

This paper was received on April 7, 1978.

non-flow gas laser equations when the flow speed approaches zero.

The introduction of thermal velocity distribution to the speed equation will enable us to obtain the theoretical relations between the gain, intensity and power of gas flow lasers. When the flow speed equals zero, these relations reduce to the familiar non-flow gas laser equations. Under uniform broadening, the results are the same as those reported in references [1,2]. It must be pointed out that, vigorously speaking, particle thermal velocity distribution cannot be brought into the speed equations. However, this technique very simply provided desirable results and will serve as a basis for further analysis.

## II. ASSUMPTIONS AND BASIC EQUATIONS

Let us assume the following: The optical axis is perpendicular to the direction of gas-flow, gas passage is rectangular in cross-section and plane parallel mirrors are placed on either side of the passage as shown in Figure 1. The variations of gas parameters  $u$ ,  $p$  and  $T$  inside the optical chamber can be neglected. The effect of the boundary layer is also negligible [7].

The pump region and the optical chamber are separated in order to analyze the "flow broadening" pulse width of the pulsed pump upstream of the optical chamber.

The working energy levels of the  $\text{CO}_2\text{-N}_2$  laser system can be described as the five-energy level model shown in Figure 2. Energy level 1 includes the symmetric and bending levels of  $\text{CO}_2$ . The number of particles transported from energy level  $i$  to  $j$ , due to inelastic collisions, in a unit time is  $K_{ij}N_i$ ;  $N_i$  is the density of particles at energy level  $i$ . Speed  $K_{ij}$  (unit  $\text{sec}^{-1}$ ) satisfies the following:

$$K_u, K_n, K_{\nu} \gg K_{ii} > K_{ij} (i = 1, 2, 3) \quad (2.1)$$

With constant  $u$ ,  $p$  and  $T$ , the non-constant speed equations and the radiation exchange equation are:

$$\left. \begin{aligned} \frac{\partial N_1}{\partial t} + u \frac{\partial N_1}{\partial x} &= \omega_1 - K_{10}N_1 + K_{21}N_2, \\ \frac{\partial N_2}{\partial t} + u \frac{\partial N_2}{\partial x} &= \omega_2 + K_{21}N_1 - (K_{10} + K_{22})N_2 - \frac{J}{ch \nu} (B'_{11}f_1N_1 - B'_{21}f_2N_2) \\ \frac{\partial N_3}{\partial t} + u \frac{\partial N_3}{\partial x} &= \omega_3 + K_{22}N_2 - K_{10}N_1 + \frac{J}{ch \nu} (B'_{22}f_2N_2 - B'_{12}f_1N_1) \end{aligned} \right\} \quad (2.2)$$

$$N_1 + N_2 + N_3 = \text{常数}$$

$$N_{e'} + N_1 = \text{常数}$$

$$\frac{\partial J}{\partial t} + c \text{grad } J = (B'_{21}f_2N_2 - B'_{12}f_1N_1)J \quad (2.3)$$

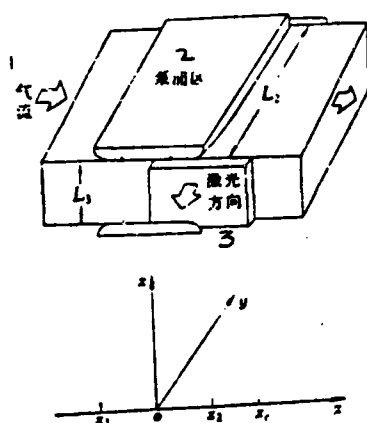


Figure 1. Schematic diagram of a transverse gas flow laser and coordinate system.

(pump zone  $x_1 \leq x \leq x_2$ ; optical chamber  $0 \leq x \leq x_3 = L$ )

1—gas flow; 2—pump zone;  
3—laser direction

where  $t$  is time,  $u$  is flow-speed,  $\omega_i$  ( $i=1,2,3$ ) is pump speed;  $c$  is speed of light,  $h$  is the Boltzmann constant,  $\nu$  is light frequency,  $J$  is radiation intensity;  $f_i$  ( $i=1,2$ ) is the fraction of particles in  $N_i$  with laser action,  $B'_{11}$  is the speed of excited particles with Doppler frequency  $\nu'$  under the influence of radiation with frequency  $\nu$ .

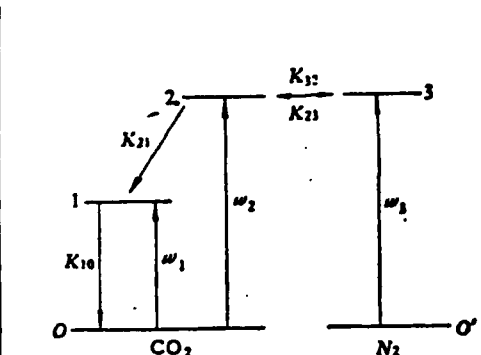


Figure 2. Energy levels of the  $\text{CO}_2-\text{N}_2$  laser system and relaxation processes.

$$B'_n = B_n \frac{2/\pi \Delta \nu_N}{1 + \left[ \frac{2(\nu' - \nu)}{\Delta \nu_N} \right]^2}, \quad B'_u = \frac{g_1}{g_2} B'_n \quad (2.4)$$

$g_i$  ( $i=1, 2$ ) is the statistical weight of energy level;  $\Delta \nu_N$  is the full width at half peak of the uniform broadening curve.  $I$  is the direction of light propagation. The intensity satisfies the following boundary conditions

$$\left. \begin{array}{l} y = 0, J_0^+ = R_1 J_0^-, R_1 = 1 - a_1 - t_1 \\ y = L, J_L^+ = R_2 J_L^-, R_2 = 1 - a_2 - t_2 \end{array} \right\} \quad (2.5)$$

$R_i$ ,  $a_i$  and  $t_i$  ( $i=1, 2$ ) are the reflection, absorption and transmission coefficients of the mirrors on both sides respectively.  $J^+$  and  $J^-$  are the photon energy flows in the positive and negative  $y$  direction and we have  $J = J^+ + J^-$ .

### III. SOLUTION

On the left hand of (2.3), with the exception of  $\frac{\partial J}{\partial y}$  other terms are small enough to be negligible. Therefore, from (2.3) and (2.5), we get

$$g = \frac{1}{L} \int_0^L \frac{1}{c} (B'_n f_1 N_1 - B'_u f_1 N_1) dy = \frac{-1}{2L} \ln R_1 R_2 \quad (3.1)$$

Because [1]  $J_{\max}/J_{\min} = 2\sqrt{R}/(1+R)$ ,  $R = \min(R_1, R_2)$ , therefore, the variation of  $J$  along the  $y$  direction can be neglected when  $R \leq 0.6$ . From (2.3) and (2.5), we obtain

$$gI = \frac{1}{L} \int_0^L \frac{1}{c} (B'_n f_1 N_1 - B'_u f_1 N_1) J dy = \frac{1}{L} (J_L^+ - J_L^- + J_0^- - J_0^+) \quad (3.2)$$

$$J_0 = J_0^- (1 + R_1) = \frac{gI L (1 + R_1) \sqrt{R_1}}{(\sqrt{R_1} + \sqrt{R_2})(1 - \sqrt{R_1 R_2})}, \quad I = \frac{1}{L} \int_0^L J dy \quad (3.3)$$

The  $g$  here is the average gain coefficient with respect to  $y$ . Equation (3.1) is the condition required for gas flow laser resonance. Generally,  $R_i$  and  $g$  vary with  $x$ .

The solution to the speed equations is obtained as follows:  
First take the integral average of (2.1) with respect to  $y$  and  
then carry out these mathematical transformations:

$$\xi = \frac{x}{u}, \quad \zeta = \epsilon - \frac{x}{u} \quad (3.4)$$

(2.1) is then changed into:

$$\left. \begin{aligned} \frac{\partial^2 n_b}{\partial \xi^2} + (K_{12} + S_1 K_{21} + S_2 K_{10}) \frac{\partial n_b}{\partial \xi} + S_2 K_{12} K_{10} n_b \\ = K_{12} \sum_{i=1}^3 w_i + \frac{\partial(\omega_1 + \omega_2)}{\partial \xi} + S_0 \left[ (K_{10} - K_{21}) \frac{\partial g}{\partial \xi} + K_{12} K_{10} g \right] \\ \frac{\partial^2 n_s}{\partial \xi^2} + (K_{12} + S_1 K_{21} + S_2 K_{10}) \frac{\partial n_s}{\partial \xi} + S_2 K_{12} K_{10} n_s \\ = S_1 K_{21} \sum_{i=1}^3 w_i + S_2 K_{10} w_3 + \frac{\partial w_3}{\partial \xi} + S_0 K_{21} \left( \frac{\partial g}{\partial \xi} + K_{10} g \right) \end{aligned} \right\} \quad (3.5)$$

where

$$n_b = n_1 + n_2, \quad n_s = S_1 n_b + S_0 g, \quad n_i = S_2 n_b - S_0 g \quad (3.6)$$

$$S_0 = \frac{c}{B'_{11}f_2 + B'_{12}f_1}, \quad S_1 = \frac{B'_{12}f_1}{B'_{11}f_2 + B'_{12}f_1}, \quad S_1 + S_2 = 1 \quad (3.7)$$

$$n_i = \frac{1}{L_1} \int_0^{L_1} N_i dy$$

Let  $g = g(\zeta) e^{st}$ , and then obtain the solution to (3.5) as:

$$\left. \begin{aligned} n_b = n_{b0} + S_0 g n_{bs} + \sum_{\substack{i=1 \\ i \neq 1, 2}}^3 \frac{e^{-\lambda_i t}}{\lambda_i - \lambda_1} \{ (\omega_1 + \omega_2 - \lambda_i n_{bs}) + K_{12} n_i^0(\zeta) \\ + (\lambda_i - S_1 K_{21} - S_2 K_{10}) n_i^0(\zeta) + S_0 g [(K_{10} - K_{21}) - (\lambda_i + \delta) n_{bs}] e^{-st} \} \\ n_s = n_{s0} + S_0 g n_{ss} + \sum_{\substack{i=1 \\ i \neq 1, 2}}^3 \frac{e^{-\lambda_i t}}{\lambda_i - \lambda_1} \{ (\omega_1 - \lambda_i n_{ss}) + (\lambda_i - K_{10}) n_i^0(\zeta) \\ + S_1 K_{21} n_i^0(\zeta) + S_0 g [K_{10} - (\lambda_i + \delta) n_{ss}] e^{-st} \} \end{aligned} \right\} \quad (3.8)$$

The superscript 0 on the right represents the distribution of the corresponding quantity at  $\xi = 0$  (i.e.,  $x=0$ ).  $\delta$  is a constant and  $w_1$  is another constant.

$$\lambda_{1,2} = \frac{1}{2} \{ (K_{12} + S_1 K_{21} + S_2 K_{10}) \pm \sqrt{(K_{12} + S_1 K_{21} + S_2 K_{10})^2 - 4 S_2 K_{12} K_{10}} \}$$

$$n_{1s} = \frac{(K_{10} - K_{20})\delta + K_{12}K_{10}}{\delta^2 + (K_{12} + S_1K_{20} + S_2K_{10})\delta + S_2K_{12}K_{10}},$$

$$n_{2s} = \frac{K_{20}(K_{10} + \delta)}{\delta^2 + (K_{12} + S_1K_{20} + S_2K_{10})\delta + S_2K_{12}K_{10}}$$

$$n_{1p} = \begin{cases} \frac{1}{S_2K_{10}} \sum_{i=1}^3 \omega_i, & 0 \leq \xi \leq \xi_1 = \frac{x_1}{u} > 0 \\ 0, & \xi > \xi_1 \end{cases}$$

$$n_{2p} = \begin{cases} \frac{S_2K_{10}\omega_1 + S_1K_{20} \sum_{i=1}^3 \omega_i}{S_2K_{12}K_{10}}, & 0 \leq \xi \leq \xi_1 \\ 0, & \xi > \xi_1 \end{cases}$$

(3.8) is the solution when  $\lambda_1 \neq \lambda_2$ . Similarly, a solution when  $\lambda_1 = \lambda_2$  can be obtained. It will not be discussed here. The initial distribution at  $x = 0$  is explained as follows: (1) initial distribution can be obtained from the solution to (2.2) under radiationless condition  $J = 0$ . The radiationless solution is not going to be written here. Under continuous pumping at the upstream of the optical chamber,  $n_i^0(\xi)|_{\xi=0} = n_i^0(x)|_{x=0} = \text{constant}$ . When pulsed pumping is used,  $n_i^0(x)|_{x=0}$  varies with  $t$ . (2) the radiationless solution usually generally does not satisfy (3.1). However, since  $\frac{2L_2}{c(1-R_1R_2)} \ll K_{10}^{-1}, K_{20}^{-1}, \frac{n_2}{\omega_2}$ , the inelastic exchange of collision within the time period  $\frac{2L_2}{c(1-R_1R_2)}$  cannot be completed.

In addition, since  $\frac{2L_2\omega}{c(1-R_1R_2)} \ll L_2$ , at  $\xi = 0$  we get:

$$n_i^0 = n_i^0(\xi) + n_i^0(\xi), \quad n_i^0 = n_i^0(\xi) \quad (3.9)$$

where  $n_i^0(\xi) = n_i^0(x)|_{x=0} (i = 1, 2, 3)$  which can be obtained from the radiationless solution. (3) generally, since  $K_{12}, K_{10} \gg K_{11}, \frac{\omega}{L_1}$ , therefore  $K_{12}n_1^0(\xi) = K_{10}n_2^0(\xi)$ .

From (2.2) and (3.6),  $gI$  can be obtained

$$\begin{aligned} \frac{gI}{h\nu} &= S_2\omega_2 - S_1\omega_1 + S_2K_{12}n_1 - S_1f n_2 - S_0g(\delta + K_{11} + S_2K_{20} + S_1K_{10}) \\ &= \frac{2}{\pi\Delta\nu_N} \frac{K_0 I_0}{h\nu} \exp\left\{-\left[\frac{2(\nu' - \nu_0)\sqrt{\ln 2}}{\Delta\nu_N}\right]^2\right\} \\ &\quad - \left(1 + \left[\frac{2(\nu' - \nu)}{\Delta\nu_N}\right]^2\right) \frac{gI}{h\nu} \end{aligned} \quad (3.10)$$

where

$$f = K_{21} + S_2 K_{23} - S_3 K_{10} \quad (3.10)_1$$

$$\begin{aligned} \frac{2}{\pi \Delta \nu_N} \frac{K_0 I_s}{h\nu} &= \left( \omega_{20} + \omega_{30} - \frac{S_1 K_{23}}{S_2 K_{10}} \sum_{i=1}^3 \omega_{i0} \right) + \sum_{\substack{i=1, j=2 \\ j=1, 3}}^2 \frac{e^{i\lambda_i \xi}}{\lambda_i - \lambda_j} \{ S_2 K_{12} (\omega_{30} - \lambda_i n_{i0}) \right. \\ &\quad - S_1 f (\omega_{10} + \omega_{20} - \lambda_i n_{i0}) + [S_2 K_{12} (\lambda_i - K_{32}) - S_1 f K_{32}] n_{30}^0(\xi) \\ &\quad \left. + [S_1 S_2 K_{12} K_{32} - S_1 f (\lambda_i - S_1 K_{23} - S_2 K_{10})] n_{10}^0(\xi) \} \\ \frac{I_s}{h\nu} &= \frac{\pi \Delta \nu_N}{2} \frac{c S_1}{B_{21} f_2} \left\{ (K_{21} + S_2 K_{23} + S_3 K_{10} + \delta - S_3 K_{12} n_{10} + S_1 f n_{20}) \right. \\ &\quad - \sum_{\substack{i=1, j=2 \\ j=1, 3}}^2 \frac{e^{-(\lambda_i + \delta) \xi}}{\lambda_i - \lambda_j} (S_2 K_{12} [K_{32} - (\lambda_i + \delta) n_{10}] - S_1 f [K_{10} - K_{20}] \right. \\ &\quad \left. \left. - (\lambda_i + \delta) n_{20}] \right\} \right\} \end{aligned}$$

In the derivation of (3.10), it has been assumed that a quasi-equilibrium was reached and partial Maxwell velocity distribution was established, i.e.,

$$\begin{aligned} \omega_i &= \omega_{i0} \exp \left\{ - \left[ \frac{2(\nu' - \nu_0) \sqrt{\ln 2}}{\Delta \nu_D} \right]^2 \right\}, \\ n_i &= n_{i0} \exp \left\{ - \left[ \frac{2(\nu' - \nu_0) \sqrt{\ln 2}}{\Delta \nu_D} \right]^2 \right\} \end{aligned}$$

where  $\nu_0$  is the center frequency of the Doppler line and  $\Delta \nu_D$  is the full width at half peak in the Doppler line.

#### IV. GAIN, INTENSITY AND POWER

Using (3.10) under conditions that the light frequency equals the Doppler center frequency (i.e.,  $\nu = \nu_0$ ), we get

$$g = \frac{K_0}{\pi} \int_{-\infty}^{\infty} \frac{\exp(-z^2 \eta^2)}{1 + z^2 + I/I_s} dz = \frac{K_0 \exp \left[ \eta^2 \left( 1 + \frac{I}{I_s} \right) \right]}{\sqrt{1 + I/I_s}} \left\{ 1 - \text{erf} \left( \eta \sqrt{1 + \frac{I}{I_s}} \right) \right\} \quad (4.1)$$

where  $\eta = \frac{\Delta \nu_N}{\Delta \nu_D} \sqrt{\ln 2}$ ,  $z = \frac{2(\nu' - \nu_0)}{\Delta \nu_N}$ ,  $\text{erf}$  is the probability integral. When non-uniform broadening dominates, i.e.,  $n \rightarrow 0$ , (4.1) becomes

$$g = \frac{K_0(\xi, \zeta)}{\sqrt{1 + I/I_s(\xi)}} \quad (4.2)$$

When uniform broadening dominates, i.e.,  $\eta \rightarrow \infty$  (4.1) becomes

$$g = \frac{g_0(\xi, \zeta)}{1 + I/I_0(\xi)}, \quad g_0 = \frac{K_0}{\eta \sqrt{\pi}} \quad (4.3)$$

It is defined as the partial saturation intensity  $K_0$  and  $g_0$  are non-uniform and uniform broadening saturation gain coefficients, respectively. When the gain is equal to the loss, the above equation also applies. It becomes the familiar theory [6] on non-flow gas lasers. When  $\lambda, \xi \gg 1$

$$I_s \rightarrow \bar{I}_s = \frac{\pi \Delta \nu_N}{2} \frac{c h \nu S_2 K_{11} K_{12} K_{10} + \delta [K_{11} K_{12} + (K_{11} + K_{12} + K_{10}) K_{10}]}{S_2 K_{12} K_{10} + (K_{11} + S_1 K_{12} + S_2 K_{10}) \delta} \quad (4.4)$$

$$K_0 I_s \rightarrow \bar{K}_0 \bar{I}_s = \frac{\pi \Delta \nu_N h \nu}{2} \left( \omega_{20} + \omega_{30} - \frac{S_1 K_{11}}{S_2 K_{10}} \sum_{i=0}^3 \omega_{i0} \right)$$

Equation (4.4) omits  $\delta^2$  as a higher order term. From (4.1)-(4.3), it is easy to obtain the radiation intensity in the optical chamber. The transmitted intensity  $J_t$  is

$$J_t = J_{s1}^- + J_{s2}^+ = \frac{g_0 I L_2 (\epsilon_1 \sqrt{R_2} + \epsilon_2 \sqrt{R_1})}{(\sqrt{R_1} + \sqrt{R_2})(1 - \sqrt{R_1 R_2})} \quad (4.5)$$

Integrating  $J_t$  with respect to  $x$  and  $t$ , we get the power. For single end output with the other end as a no-loss total reflection mirror (i.e.,  $R_2 = 1$ ), we get

$$P = \frac{V}{L_1(\xi - \xi_0)} \int_{\xi_0}^{\xi} \int_{\epsilon_0}^{\epsilon_1} \frac{\epsilon_1 u}{a_1 + \epsilon_1} \frac{K_0 I \exp \left[ \eta^2 \left( 1 + \frac{I}{I_s} \right) \right]}{\sqrt{1 + I/I_s}} \left[ 1 - \operatorname{erf} \left( \eta \sqrt{1 + \frac{I}{I_s}} \right) \right] d\xi d\epsilon \quad (4.6)$$

where  $V = L_1 L_2 L_3$  is the volume of the optical chamber. For  $\eta \gg 1$ , (4.6) becomes

$$P = \frac{u V \epsilon_1}{L_1(\xi - \xi_0)(a_1 + \epsilon_1)} \left\{ \int_{\xi_0}^{\xi} \int_{\epsilon_0}^{\epsilon_1} g_0 I d\xi d\epsilon \Big|_{\epsilon=0} + \frac{\ln R^0}{L_2} \int_{\xi_0}^{\xi} \int_{\epsilon_0}^{\epsilon_1} I_s e^{\epsilon I_s} d\xi d\epsilon \Big|_{\epsilon=0} \right\}$$

$$= \frac{\epsilon_1 V I_s^0}{L_1(a_1 + \epsilon_1)} (g_0^* L_2 + \ln R^0) \quad (4.7)$$

where

$$I_s^0 = \frac{u}{L_1(\xi - \xi_0)} \int_{\xi_0}^{\xi} \int_{\epsilon_0}^{\epsilon_1} I_s e^{\epsilon I_s} d\xi d\epsilon \Big|_{\epsilon=0},$$

$$g_0^* L_2 = \frac{L_2 \int_{\xi_0}^{\xi} \int_{\epsilon_0}^{\epsilon_1} g_0 I d\xi d\epsilon \Big|_{\epsilon=0}}{\int_{\xi_0}^{\xi} \int_{\epsilon_0}^{\epsilon_1} I_s e^{\epsilon I_s} d\xi d\epsilon \Big|_{\epsilon=0}} \quad (4.8)$$

$I_s^*$  and  $g_o^*$  can be considered as the gain coefficients of uniform saturation intensity and non-uniform saturation intensity, respectively. They are average values with respect to time and space. (4.7) is in the same form as the Rigrod equation for non-flow gas lasers. Substituting (3.10) into (4.8),  $I_s^*$  and  $g_o^*$  can be obtained:

$$I_s^* = \frac{\pi \Delta \nu N}{2 B_{11} L_1} \frac{ch \nu u S_1}{L_1} \left\{ (K_{11} + S_1 K_{21} + S_1 K_{10} + \delta - S_1 K_{12} n_{12} + S_1 f n_{bs}) \frac{e^{iL_1/\eta} - 1}{\delta} \right. \\ \left. - \sum_{i=1}^2 \frac{1 - e^{-iL_1/\eta}}{\lambda_i (\lambda_i - \lambda_s)} (S_1 K_{12} [K_{12} - (\lambda_i + \delta) n_{12}] \right. \\ \left. - S_1 f [(K_{10} - K_{21}) - (\lambda_i + \delta) n_{bs}]) \right\} \quad (4.9)$$

The expression for  $g_o^*$  is going to be omitted. The  $t_1^*$  corresponding to the maximum power out is obtained based on  $\frac{\partial P}{\partial t_1} = 0$ . For  $\delta = 0$ , we get

$$\frac{t_1^*}{a_1} = \frac{1 - a_1 - t_1^*}{a_1 + t_1^*} [g_o^* L_1 + \ln(1 - a_1 - t_1^*)] \quad (4.10)$$

From (4.7) and (4.10), the maximum power output  $P^*$  is

$$P^* = \frac{V I_s^* (t_1^*)^2}{L_1 a_1 (1 - a_1 - t_1^*)} = \frac{(t_1^*)^2}{a_1 (1 - a_1 - t_1^*)} \frac{u V}{L_1 L_2 (\zeta - \zeta_o)} \int_{\zeta_o}^{\zeta} \int_0^{t_1^*} I_s d\zeta dt_1 \Big|_{t_1^*} \quad (4.11)$$

The above equation has the same form as the Rigrod equation [6]. For  $\eta \ll 1$  (non-uniform broadening), the same discussion can be made.

## V. ANALYSIS OF PARAMETERS

$I_s$  is proportional to the square of the pressure  $P^2$ . It is not related to the pumping rate and the degree of excitation of the gas at the inlet of the optical chamber. From (3.10) we know that  $I_s$  decreases monotonically with  $\frac{x}{u}$  from its maximum  $I_s$

max at  $x = 0$  to  $\bar{I}_s$  (see equation (4.4)).

$$I_{s,\max} = I_s|_{x=0} = (K_{21} + S_2 K_{22} + S_1 K_{10} + \delta) \frac{\cosh \nu S_2}{B_{21} f_2} \frac{\pi \Delta \nu_N}{2} \quad (5.1)$$

Increasing the flow speed (leaving other parameters unchanged), we found that  $I_{s,\max}$  remained the same but  $I_s$  and  $\bar{I}_s$  increased significantly (see example). The variation in reflectivity  $R_1 = (R_1^0)^{\delta \xi}$  significantly affects  $I_s$ . The reasonable limits for  $\delta$  was derived to be:

$$|\delta| < \min(\lambda_1, \lambda_2) \text{ for } |\delta| = O(K_{21}) \quad (5.2)$$

From (4.4) we know that  $\delta \approx -\frac{K_{21} K_{22}}{K_{21} + K_{22}}$ ,  $\bar{I}_s \approx 0$ . This is because when  $\delta < 0$   $R_1$  increases monotonically with  $\frac{x}{u}$  and  $t_1$  monotonically decreases. When  $t_1$  is reduced to zero, light radiation is forced to stop; when  $\delta > 0$   $I_s|_{t_1=0} > \text{or} \gg \bar{I}_s|_{t_1=0}$ . In gas-flow lasers,  $K_0$  and  $g_0$  are parameters of  $I_s$  which are related to the mirror surface conditions. Only when  $u = 0$  and  $\delta = 0$ , these parameters will have the physical meaning of corresponding parameters for non-flow steady-state gas lasers. It demonstrates the characteristics of the non-steady state nature of gas-flow lasers. The parametric dependence of  $I_s^*$  is identical to that of  $I_s$ .

If the pumping rate  $w_i$  is proportional to  $p$ , then the non-saturation gain coefficient  $K_0$  is not related to  $p$  and  $g_0$  is inversely proportional to  $p$ .  $K_0$ ,  $g_0$  and  $w_i$  are proportional to the degree of excitation of the gas at the inlet of the optical chamber. From (3.10) and (4.4), we know that for pumping upstream of the optical chamber, for  $\delta \geq 0$ ,  $g_0$  decreases monotonically and for  $\delta < 0$ ,  $g_0$  increases monotonically. For pumping inside the optical chamber, we get from (4.4)

$$\bar{K}_0 = \left( w_{21} + w_{22} - \frac{S_1 K_{21}}{S_2 K_{10}} \sum_{i=1}^3 w_{i0} \right) \cdot \frac{B_{21} f_2 [S_2 K_{22} K_{10} + (K_{21} + S_2 K_{22} + S_1 K_{10}) \delta]}{c S_2 \{K_{21} K_{22} K_{10} + [K_{21} K_{22} + (K_{21} + K_{22} + K_{10}) K_{10}] \delta\}} \quad (5.3)$$

Therefore, for the same pumping conditions,  $\bar{K}_0|_{s>0} < (\text{or } \ll) \bar{K}_0|_{s=0}$ .

Power P is proportional to p, u, pumping speed and the degree of excitation at the inlet of the optical chamber. When reflectivity is constant and  $\delta = 0$ , the maximum power output  $P^*$  is proportional to  $p^2$  and mirror area.

## VI. EXAMPLE

For a  $\text{CO}_2/\text{N}_2/\text{He}$  gas mixture, the speed constants are tabulated as follows [8]:

speed constants at  $T = 300^\circ\text{K}$

$\text{N}_{\text{He}}/\text{N}$	$K_{10}/p$ (TORR $^{-1}$ sec $^{-1}$ )	$K_{21}/p$ (TORR $^{-1}$ sec $^{-1}$ )	$K_{23}/p$ (TORR $^{-1}$ sec $^{-1}$ )	$K_{32}/K_{23}$
0	$8.8 \times 10^2$	$1.23 \times 10^2$	$1.67 \times 10^4$	
0.3	$1.2 \times 10^3$	$1.03 \times 10^2$	$1.16 \times 10^4$	
0.5	$1.9 \times 10^3$	$9.6 \times 10^1$	$8.3 \times 10^4$	$\text{N}_{\text{CO}_2}/\text{N}_{\text{N}_2}$

From information in reference [8], we get

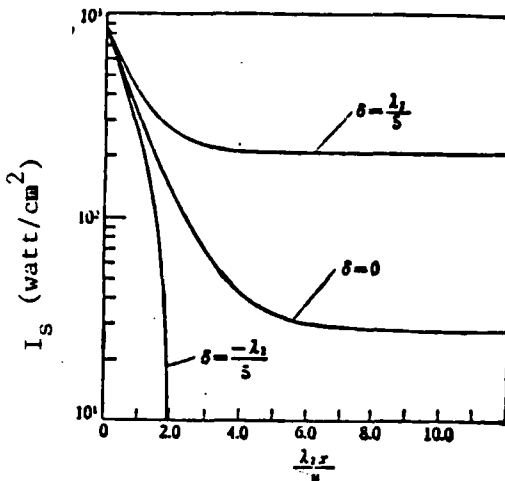
$$\frac{S_1}{S_0} = \frac{\lambda_0 \theta}{4\pi \tau_{21} \nu_e} \frac{2(2l+1)}{T} \cdot \exp\left[-l(l+1) \frac{\theta}{T}\right] \approx \frac{718}{NT} (\text{cm}^2)$$

$S_1/S_2$  is also a function of temperature and degree of excitation. When  $T = 300^\circ\text{K}$  and degree of excitation is not too high,  $\frac{S_1}{S_2} \approx 0.04$ .

The variation of  $I_s$  with  $\lambda$  ( $\lambda_s < \lambda_0$ ) is shown in Figure 3.  $I_s$  approximately is in the  $10^3 - 10^4$  watt/cm $^2$  region which is consistent with experimental results. The calculated curve of  $I_s$  proved the analytical conclusion given in the previous section. When  $\delta = \frac{\lambda_s}{\lambda_0}$ ,  $I_s$  is 10 times larger than  $I_s|_{s=0}$ .

Figure 3. Variation of  $I_s$  with  $\frac{\lambda_x}{u}$

$T = 300K, \rho = 30, \text{CO}_2/\text{N}_2/\text{He} = 1/4/5$



Figures 4 and 5 show the change of  $g_o$  and  $I$  with  $\frac{\lambda_x}{u}$  and  $\frac{u}{L_1}$ , respectively. The pulsing time of the pump vs. time can be expressed as the variation of  $n_2^0$  with  $\frac{u}{L_1}$ .  $g_o$  and  $I$  are like "waves" propagating in the right direction. Straight lines  $\frac{u}{L_1} - b \frac{\lambda_x}{u} = 0$  and  $= 1$  are the front and back surfaces of the wave where  $b = \frac{u}{L_1}$ . From Figures 4 and 5, we know that along a straight line  $\frac{u}{L_1} - b \frac{\lambda_x}{u} = H = \text{const} < H < 1$ , the variation of  $g_o$  is slower than that of  $I$ .

For continuous pumping, when  $R_1 = \text{const}$ ,  $\bar{g}_o^*$  monotonically gradually decreases with  $\frac{\lambda_x}{u}$ . When  $\frac{\lambda_x}{u} = 10$ ,  $\bar{g}_o^*$  is approximately 0.8. When  $\delta = \frac{\lambda_2}{s}$ ,  $\bar{g}_o^*$  more significantly monotonically declines. When  $\frac{\lambda_x}{u} = 10$ ,  $\bar{g}_o^*$  is about 0.1. When  $\delta = -\frac{\lambda_1}{s}$ ,  $\bar{g}_o^*$  increases with  $\frac{\lambda_x}{u}$  and  $I_s^*$  decreases with  $\frac{\lambda_x}{u}$ . Note that  $\bar{g}_o^*$  and  $I_s^*$  do not have any obvious physical meanings. From Figures 4 and 6, it can be seen that when  $R$  is constant, the variations of  $g_o$  and  $g_o^*$  with  $\frac{x}{u}$  are slow regardless of whether continuous or pulsed pumping is used. This serves as a theoretical basis for the calculation of gas flow laser power using an average value of the gain coefficient and the non-flow gas laser equation as suggested in references [5,7].

Gas laser power calculated here agrees with that reported in reference [1] (see Figure 7).  $\frac{\lambda_x}{u}$  represents the fraction of effective vibrational energy taken. For the calculation parameters in Figure 7, when  $\frac{\lambda_x}{u} \approx 5$ , the effective energy is completely used.

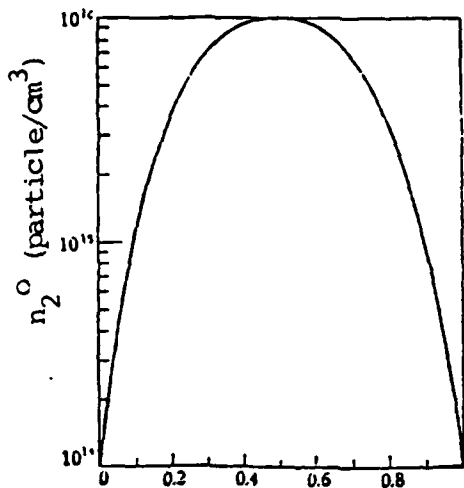


Figure 4.1. The variation of  $n_2^0$  with  $\frac{u/L_1}{u/L_1}$  at inlet of optical chamber.

$T = 300\text{K}$ ,  $p = 30$  torr,  $\delta = 0$ ,  $g_{\text{abs}} = 2 \times 10^{-3} \text{cm}^{-1}$ ,  
 $\text{CO}_2/\text{N}_2/\text{He} = 1/4/5$

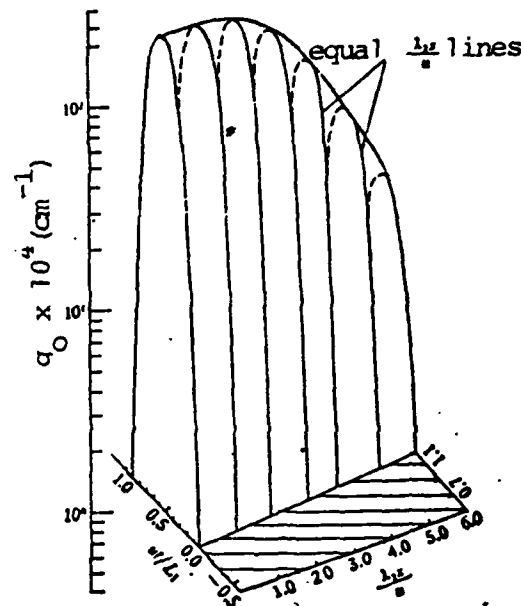


Figure 4.  $g_0 \times 10^4$  vs.  $\frac{\lambda_2 x}{u}$  and  $\frac{u}{L_1}$  curves.

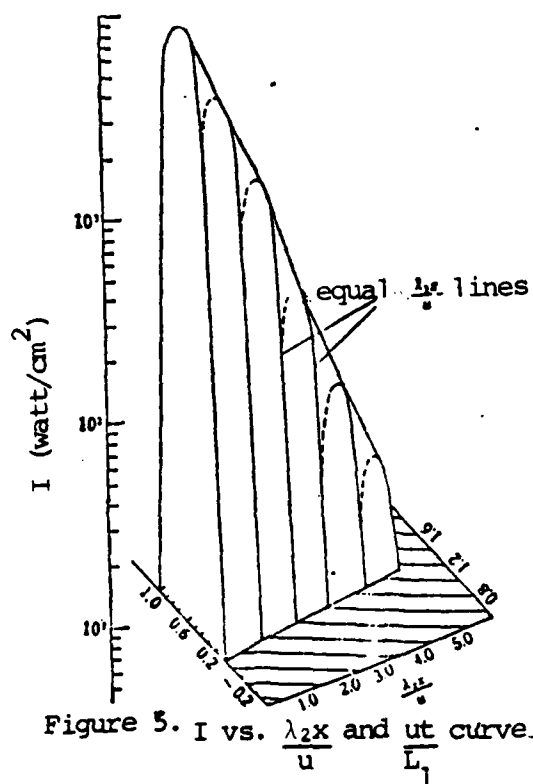


Figure 5.  $I$  vs.  $\frac{\lambda_2 x}{u}$  and  $\frac{u}{L_1}$  curve.

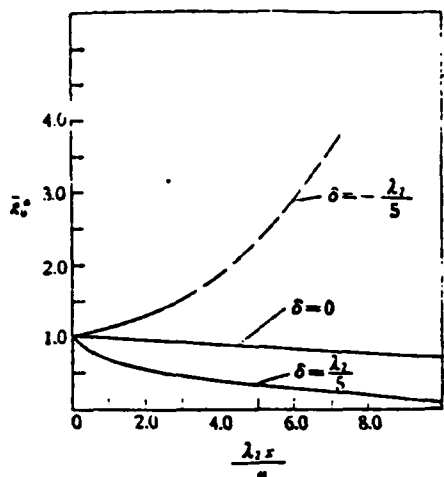


Figure 6. Unified average non-saturation gain  $g_0^*$  vs.  $\frac{\lambda_2 x}{u}$

$T=300^\circ K$   $p=30$  torr  
 $CO_2/N_2/He=1/4/5$

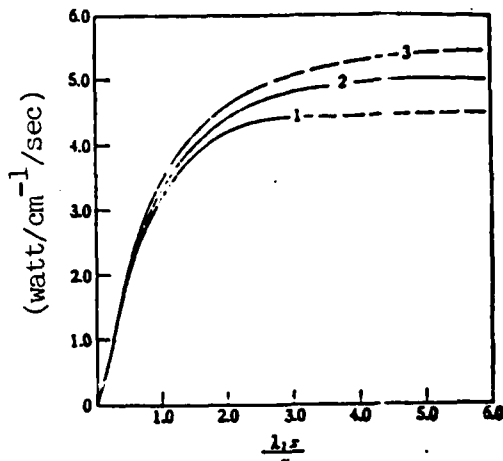


Figure 7. Gas laser output power  $p_uA$  vs.  $\frac{\lambda_2 x}{u}$

1.  $\delta = \frac{\lambda_2}{5}$ , 2.  $\delta = 0$ , 3.  $\delta = -\frac{\lambda_1}{5}$ ,  
 $T=300^\circ K$ ,  $p=30$  torr  
 $CO_2/N_2/He=1/4/5$   $\frac{\epsilon_1}{\epsilon_1 + \epsilon_2} = 0.7$ ,  
 $g_{x=0} = 2 \times 10^{-3} \text{ cm}^{-1}$   $n_2^0 = 10^{16}$   
 particle/cm<sup>3</sup>

#### REFERENCES

- [1] Cool, T. A., *J. Appl. Phys.*, **40**, 9 (1969), 3563.
- [2] Пименов, В. П., и др., *Кван. звук.*, **4**, 2 (1977), 255.
- [3] Goela, J. S., et al., *AIAA J.*, **13**, 12 (1975), 1629.
- [4] Davis, J. W., et al., *AIAA Paper*, No. 72-722.
- [5] Lee, G., et al., *AIAA J.*, **10**, 1 (1972), 65.
- [6] Maitland, A., et al., *Laser Physics*, 1969.
- [7] Kao Chi, *Physics Journal*, **27**, 4 (1978), p. 340.
- [8] Hoffman, A. I., et al., *IEEE J.*, **QE-8** (1972), 46.
- [9] Cheo, P. K., *Lasers*, **3**, Chap. 2, New York, Dekker 1968.

CONTACT PROBLEMS OF LONG RIGID  
FRAME FOOTING ON ELASTIC FOUNDATION

Zeng Xin-Chuan\*

(The Seismological Brigade of Wuhan, National  
Seismological Bureau)

In reference [1], Galin solved the contact problems between two flat bottom pressure heads under center load and elastic semi-flat foundation with friction present. The distribution of stress along the contact surface was obtained. In this paper, the author used the Muskhelishvili method [2] to attack the contact problems of long rigid frame footing under off-center load on an elastic foundation. For simplicity in the calculation, it was assumed that the contact between the footing and the foundation is frictionless.

The action of an off-center load (Figure 1) is equivalent to the combination of the actions of a center load and a force pair (Figure 2). The boundary conditions of center loading are:

$$\left. \begin{array}{lll} \tau_x = 0 & y = 0 & |x| < \infty \\ \sigma_x = 0 & y = 0 & |x| < a \quad |x| > b \\ v = c \text{ (常数)} & y = 0 & a < |x| < b \end{array} \right\} \quad (1)$$

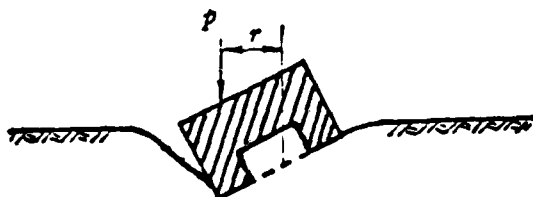


Figure 1

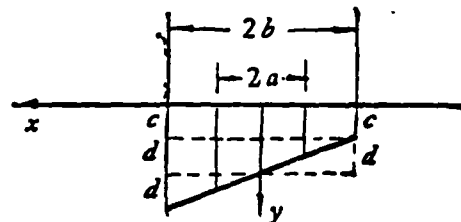


Figure 2

\*This paper was received on November 7, 1978.

For the force pair, the boundary conditions are:

$$\left. \begin{array}{lll} \tau_{xy} = 0 & y = 0 & |z| < \infty \\ \sigma_x = 0 & y = 0 & |z| < a \quad |z| > b \\ v = \frac{d}{b} x - \theta z & y = 0 & a < |z| < b \end{array} \right\} \quad (2)$$

where  $\theta = d/b$  is the rotation angle of the footing.

The displacement and stress of the foundation can be expressed by the complex function  $\phi(z)$ :

$$\left. \begin{array}{l} 2\mu(u + is) = \kappa\phi(z) + \phi(\bar{z}) + (\bar{z} - z)\overline{\phi'(z)} \\ \sigma_x - \sigma_y + 2i\tau_{xy} = -2\{(z - \bar{z})\overline{\phi''(z)} - \phi'(\bar{z}) - \overline{\phi'(z)}\} \\ \sigma_y - i\tau_{xy} = \phi'(z) - \phi'(\bar{z}) + (z - \bar{z})\overline{\phi''(z)} \end{array} \right\} \quad (3)$$

The solution of  $\phi(z)$  which satisfies the boundary condition

(1) is:  $\phi'(z) = -\frac{ipz}{2\pi X(z)}$  (4)

where  $\kappa = \frac{\lambda + 3\mu}{\lambda + \mu}$ ,  $X(z) = (z^2 - b^2)^{1/2}(z^2 - a^2)^{1/2}$ . The solution of  $\phi(z)$  which satisfies the boundary conditions (2) is

$$\phi'(z) = \frac{2\mu\theta i}{1 + \kappa} \left\{ 1 - \frac{z^2 - \frac{1}{2}(a^2 + b^2)}{X(z)} \right\} \quad (5)$$

Under center loading conditions, the displacement of the footing can be obtained from (4) and (3):

$$u|_{y=0} = \frac{(\kappa - 1)p\theta}{4\pi}, \quad v|_{y=0} = -\frac{(1 + \kappa)}{4\pi\mu} \log A \quad a < |z| < b \quad (6)$$

where  $A = (b^2 - a^2)^{1/2}$ ,  $\theta = \arctan \frac{b \sin \omega}{(b^2 \cos^2 \omega - a^2)^{1/2}}$ ,  $\omega = \arcsin \frac{(b^2 - z^2)^{1/2}}{b}$ .

For footing under the action of a force pair  $M$ , the angle of rotation is:

$$\theta = \frac{(1 + \kappa)M}{2\pi\mu(b^2 - a^2)} \quad (7)$$

The stress distribution on the bottom of the footing under center load conditions can be obtained from (4) and (3) as:

$$\left. \begin{aligned} \sigma_x|_{y=0} &= -\frac{px}{\pi(x^2 - a^2)^{1/2}(b^2 - x^2)^{1/2}} \quad a < |x| < b \\ \tau_{xy}|_{y=0} &= 0 \end{aligned} \right\} \quad (8)$$

Under the action of the force pair, from (5) and (3), we get:

$$\left. \begin{aligned} \sigma_x|_{y=0} &= \frac{2M}{\pi(b^2 - a^2)} \frac{x^2 - \frac{1}{2}(a^2 + b^2)}{(x^2 - a^2)^{1/2}(b^2 - x^2)^{1/2}} \quad a < |x| < b \\ \tau_{xy}|_{y=0} &= 0 \end{aligned} \right\} \quad (9)$$

As for the stress distribution of the foundation under center loading, we obtain the following by substituting (4) into (3):

$$\left. \begin{aligned} \sigma_x &= \frac{p}{\pi} (\rho_0^1 \rho_0^2 \rho_1^1 \rho_1^2)^{-1/2} \left[ (-A(x, y) + 1)y \cos \frac{\varphi_0^1 + \varphi_0^2 + \varphi_1^1 + \varphi_1^2}{2} \right. \\ &\quad \left. + (yB(x, y) - x) \sin \frac{\varphi_0^1 + \varphi_0^2 + \varphi_1^1 + \varphi_1^2}{2} \right] \\ \sigma_y &= \frac{p}{\pi} (\rho_0^1 \rho_0^2 \rho_1^1 \rho_1^2)^{-1/2} \left[ (A(x, y) + 1)y \cos \frac{\varphi_0^1 + \varphi_0^2 + \varphi_1^1 + \varphi_1^2}{2} \right. \\ &\quad \left. - (yB(x, y) + x) \sin \frac{\varphi_0^1 + \varphi_0^2 + \varphi_1^1 + \varphi_1^2}{2} \right] \\ \tau_{xy} &= -\frac{py}{\pi} (\rho_0^1 \rho_0^2 \rho_1^1 \rho_1^2)^{-1/2} \left[ A(x, y) \sin \frac{\varphi_0^1 + \varphi_0^2 + \varphi_1^1 + \varphi_1^2}{2} \right. \\ &\quad \left. + B(x, y) \cos \frac{\varphi_0^1 + \varphi_0^2 + \varphi_1^1 + \varphi_1^2}{2} \right] \end{aligned} \right\} \quad (10)$$

where  $\rho_0^1 = [(x - a)^2 + y^2]^{1/2}$      $\rho_0^2 = [(x + a)^2 + y^2]^{1/2}$   
 $\varphi_0^1 = \arctg \frac{y}{x - a}$      $\varphi_0^2 = \arctg \frac{y}{x + a}$      $\rho_1^1 = [(x - b)^2 + y^2]^{1/2}$      $\rho_1^2 = [(x + b)^2 + y^2]^{1/2}$   
 $\varphi_1^1 = \arctg \frac{y}{x - b}$      $\varphi_1^2 = \arctg \frac{y}{x + b}$      $\left. \right\} \quad (11)$

$$\left. \begin{aligned} \rho_1^1 &= [(x - b)^2 + y^2]^{1/2} \quad \rho_1^2 = [(x + b)^2 + y^2]^{1/2} \\ \varphi_1^1 &= \arctg \frac{y}{x - b} \quad \varphi_1^2 = \arctg \frac{y}{x + b} \end{aligned} \right\} \quad (12)$$

$$\left. \begin{aligned} A(x, y) &= [(x^2 - y^2 - b^2)(x^2 - y^2 - a^2) - 4x^2y^2][(x^2 - y^2)^2 - 4x^2y^2 - a^2b^2] \\ &\quad + 8x^2y^2(x^2 - y^2)[2(x^2 - y^2) - (a^2 + b^2)]/[(x^2 + y^2)^2 \\ &\quad - 2(x^2 - y^2)b^2 + b^4][(x^2 + y^2)^2 - 2(x^2 - y^2)a^2 + a^4] \\ B(x, y) &= 2xy[(a^2 + b^2)(x^2 + y^2)^2 - 4a^2b^2(x^2 - y^2) + a^2b^2(a^2 + b^2)]/ \\ &\quad [(x^2 + y^2)^2 - 2(x^2 - y^2)b^2 + b^4][(x^2 + y^2)^2 - 2(x^2 - y^2)a^2 + a^4] \end{aligned} \right\} \quad (13)$$

Under the action of the force pair, we get the following by substituting (5) into (3):

$$\begin{aligned}
 \sigma_x &= \frac{M}{\pi(b^2 - a^2)} (\rho_0^2 \rho_0^2 \rho_1^2 \rho_1^2)^{-1/2} \left\{ [(b^2 - a^2)^2 C(x, y) - 4x] y \cos \frac{\varphi_0^1 + \varphi_0^2 + \varphi_1^1 + \varphi_1^2}{2} \right. \\
 &\quad \left. + \left[ 2\left(x^2 - y^2 - \frac{1}{2}(a^2 + b^2)\right) - (b^2 - a^2)^2 y D(x, y) \right] \sin \frac{\varphi_0^1 + \varphi_0^2 + \varphi_1^1 + \varphi_1^2}{2} \right\} \\
 \sigma_y &= - \frac{M}{\pi(b^2 - a^2)} (\rho_0^2 \rho_0^2 \rho_1^2 \rho_1^2)^{-1/2} \left\{ [(b^2 - a^2)^2 C(x, y) + 4x] y \cos \frac{\varphi_0^1 + \varphi_0^2 + \varphi_1^1 + \varphi_1^2}{2} \right. \\
 &\quad \left. - \left[ 2\left(x^2 - y^2 - \frac{1}{2}(a^2 + b^2)\right) + (b^2 - a^2)^2 y D(x, y) \right] \sin \frac{\varphi_0^1 + \varphi_0^2 + \varphi_1^1 + \varphi_1^2}{2} \right\} \\
 \tau_{xy} &= \frac{M(b^2 - a^2)}{\pi} (\rho_0^2 \rho_0^2 \rho_1^2 \rho_1^2)^{-1/2} y \left[ C(x, y) \sin \frac{\varphi_0^1 + \varphi_0^2 + \varphi_1^1 + \varphi_1^2}{2} \right. \\
 &\quad \left. + D(x, y) \cos \frac{\varphi_0^1 + \varphi_0^2 + \varphi_1^1 + \varphi_1^2}{2} \right]
 \end{aligned} \tag{14}$$

where

$$\begin{aligned}
 C(x, y) &= \frac{x[(x^2 - y^2)^2 - 4y^4 - (x^2 + y^2)(a^2 + b^2) + a^2 b^2]}{[(x^2 - y^2 - b^2)^2 + 4x^2 y^2][(x^2 - y^2 - a^2)^2 + 4x^2 y^2]} \\
 D(x, y) &= \frac{y[4x^4 - (x^2 - y^2)^2 - (x^2 + y^2)(a^2 + b^2) - a^2 b^2]}{[(x^2 - y^2 - b^2)^2 + 4x^2 y^2][(x^2 - y^2 - a^2)^2 + 4x^2 y^2]}
 \end{aligned} \tag{15}$$

Figures 3 and 4 show the stress distribution  $\sigma_y$  on a few horizontal surfaces under center loading and force pair conditions respectively. Each figure only shows half of the entire picture. The other half of Figure 3 is symmetric to what is shown. For Figure 4, the half nut shown is asymmetric to what is presented.

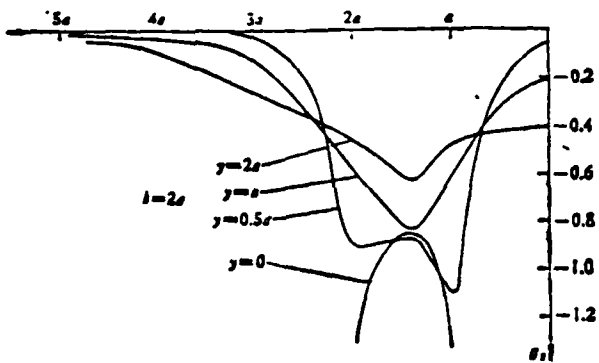


Figure 3

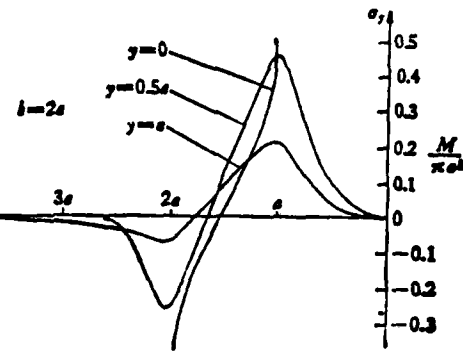


Figure 4

From (6), (7) and (8), we can see that when  $a = 0$ , the following holds for long solid rigid frame footings:

$$\begin{aligned} u|_{z=0} &= \frac{(\kappa-1)p\omega}{4\pi\mu}, & v|_{z=0} &= -\frac{(1+\kappa)p\log b}{4\pi\mu}, & |z| &< b, \\ \theta &= \frac{(1+\kappa)M}{2\pi\mu b^2}, & \sigma_z|_{z=0} &= -\frac{p}{\pi(b^2-z^2)^{1/2}}, & |z| &< b, \end{aligned}$$

Our results are consistent with those found by Galin [1], Muskhelishvili [2] and Sneddon [3].

From (9) and Figure 4, we see that  $\sigma_z|_{z=0}$  changes signs between  $-b$  and  $-a$  and  $a$  and  $b$ . This implies that tensile stress will appear at some location on the bottom of the footing. When the footing does not adhere to the foundation or when the adhesion is less than the tensile force, the footing will be detached from the foundation. Therefore, in order to avoid such a detachment effect, the load and its corresponding force pair must satisfy certain relations.

From (8) and (9), we get the stress distribution on the bottom of the footing under off-center load:

$$\sigma_z|_{z=0} = -\frac{px}{\pi(x^2-a^2)^{1/2}(b^2-x^2)^{1/2}} + \frac{2M}{\pi(b^2-a^2)} \frac{x^2 - \frac{1}{2}(a^2+b^2)}{(x^2-a^2)^{1/2}(b^2-x^2)^{1/2}}, \quad a < |z| < b$$

It is well known that in order not to allow detachment of the footing from the foundation, it is necessary to make the normal stress on the bottom of the footing be pressure stress. Therefore,

$$\frac{2M}{(b^2-a^2)} \frac{x^2 - \frac{1}{2}(a^2+b^2)}{(x^2-a^2)^{1/2}(b^2-x^2)^{1/2}} \leq \frac{px}{(x^2-a^2)^{1/2}(b^2-x^2)^{1/2}}, \quad a < |z| < b$$

and

$$M \leq p(a+b)/2 \quad (16)$$

If the action point of load is a distance  $r$  off-center (see Figure 1), then  $M = rp$ . From this the equation that  $r$  must satisfy so that the footing and the foundation will not separate is:

$$r \leq (a + b)/2 \quad (17)$$

For long solid frame footing,  $a = 0$ , and the above becomes:

$$M \leq pb/2, \quad r \leq b/2$$

This is consistent with result obtained by Muskhelishvili

#### REFERENCES

- [1] Ganin, P. A., (translated by Wang Chun Xen) "Contact Problems in Elastic Theory", Science Publication, 1958.
- [2] Muskhelishvili, N. I., *Some Basic Problems of the Mathematical Theory of Elasticity* P. Noordhoff Ltd., (1963).
- [3] Sneddon, I. N., *Fourier Transforms*, New York, McGraw-Hill, (1951).

